An assessment of GPS velocity uncertainty in California

Christopher Johnson[1], Nicholas Lau[2], and Adrian Borsa[2]

[1]UC San Diego
[2]University of California San Diego

November 21, 2022

Abstract

We analyze 580 continuous GPS stations in California from 5 analysis centers to quantify the uncertainty in published velocities and develop a composite velocity for each station. The horizontal positions are similar but the reported velocity varies by time series algorithm. Vertical rates for individual stations differ up to 5 mm/yr, with systematic differences in some areas. The published uncertainties show variability between analysis centers and are underreported, suggesting these formal errors do not reflect the true velocity uncertainties. Differences by a factor of 4 are found in the vertical and is comparable to deformation rates. An interpolated ensemble vertical velocity field is developed and regions with the highest rates of uplift or subsidence correspond to the largest variance in velocities between analysis centers, but high station density can reduce these uncertainties. Applications that rely on sub-centimeter GPS accuracy should consider the inherent uncertainty in published vertical velocity rate estimates.

An assessment of GPS velocity uncertainty in California

Christopher W. Johnson[1*], Nicholas Lau[1], and Adrian Borsa[1]

[1]Scripps Institution of Oceanography, University of California San Diego, La Jolla, California, 92093, USA

* Now at Los Alamos National Laboratory

Corresponding author: Christopher W. Johnson (cwj004@ucsd.edu)

Key Points:

- Systematic review of California GPS positions and the published and derived velocities using data from 5 different analysis centers.
- Published uncertainties show variability between analysis centers, are underreported, and do not reflect the true velocity uncertainties.
- Vertical rates for individual stations differ up to 5 mm/yr, with systematic differences in areas of highest subsidence and uplift.

Abstract

We analyze 580 continuous GPS stations in California from 5 analysis centers to quantify the uncertainty in published velocities and develop a composite velocity for each station. The horizontal positions are similar but the reported velocity varies by time series algorithm. Vertical rates for individual stations differ up to 5 mm/yr, with systematic differences in some areas. The published uncertainties show variability between analysis centers and are underreported, suggesting these formal errors do not reflect the true velocity uncertainties. Differences by a factor of 4 are found in the vertical and is comparable to deformation rates. An interpolated ensemble vertical velocity field is developed and regions with the highest rates of uplift or subsidence correspond to the largest variance in velocities between analysis centers, but high station density can reduce these uncertainties. Applications that rely on sub-centimeter GPS accuracy should consider the inherent uncertainty in published vertical velocity rate estimates.

Plain Language Summary

The continuous recordings from geodetic grade GPS sensors provides high resolution ground motion measurements. Multiple analysis centers process the raw GPS data into daily station positions and provide high quality data to the scientific community. Each analysis center applies different processing techniques and model corrections that produces differences in the final time series product. We analyze the GPS positions and published velocities for 5 analysis centers and develop a composite velocity dataset with uncertainties for 580 stations in California. The published positions are reevaluated to calculate a standardized velocity using 2 methods to assess if the differences arise from the underlying positions or the time series analysis. We find the horizontals positions are consistent but the vertical positions, which are an order of magnitude less, vary by analysis center and the greatest discrepancies are in areas of the largest observed subsidence. We further evaluate the vertical velocity field from all 5 analysis centers and develop an ensemble velocity field to characterize the spatially varying uncertainty. Our results demonstrate the importance of assessing position uncertainty using multiple analysis centers when informing geophysical models of observed ground motions.

1 Introduction

Global positioning system (GPS) instruments and processing techniques provide measurements with sufficient precision to quantify sub-centimeter geologic deformation (e.g. Dixon, 1991). The technological capabilities of GPS spurred efforts to design a permanent GPS network for continuous monitoring of the tectonic plate boundary in the western U.S. (Silver et al., 1998), ultimately realized by the construction of the Plate Boundary Observatory (PBO) between 2002 and 2012. The PBO network contains about 1,100 continuously recording GPS stations at a median spacing of ~20 km and contributes most of the regional geodetic observations used by the scientific community. Daily station positions and long-term velocities for these stations are freely and openly available (Blewitt et al., 2018; Herring et al., 2016), eliminating the need for user processing of raw GPS data and greatly expanding data access across multiple disciplines (EarthScope O&M Proposal; GAGE Facility Proposal). Increasing the diversity of GPS data users justifies the existence of the PBO network and demonstrates the value of the GPS infrastructure for scientific, government, and commercial activities (Leveson, 2009).

More than a decade of daily GPS observations from the PBO network have provided high-precision time series that constrain both short and long-term crustal motion in the western U.S. This dataset is dominated by a broad zone of deformation extending from the Pacific Coast to the western edge of the Rocky Mountains showing large horizontal displacements (median 21 mm/y). Strain localization on multiple faults across the region (e.g. Zeng et al., 2018) delineates crustal blocks whose tectonic motion is estimated at 10-45 mm/yr (e.g. Simpson et al., 2012). The dense station spacing and continuous recording enable quantification of spatiotemporally heterogeneous motion associated with volcanic activity, uplift and subsidence, and postseismic deformation (Hammond et al., 2016), whose vertical velocities are an order of magnitude smaller (median <1 mm/yr) than the horizontal. The largest contribution to vertical displacements in many areas is the solid earth elastic response to the hydrological cycle, which exhibits seasonality and non-stationarity from changes in terrestrial water storage (Argus et al., 2017; Borsa et al., 2014; Fu et al., 2015; Johnson et al., 2017).

Daily station positions and long-term velocities for most western U.S. stations are estimated by multiple analysis centers using different processing algorithms, reference frames, troposphere and tidal corrections, and time-series analysis techniques (Herring et al., 2016). Each analysis center provides uncertainty estimates for their data products, but formal uncertainties calculated for geodetic datasets can underestimate time-correlated error in position data and usually do not characterize variance introduced by different processing assumptions (Herring et al., 2016). Here, we leverage the published data products from 4 different analysis centers and analyze the empirical uncertainties across the dataset. We focus on GPS station velocities, since these are widely used and available. Our goals are to 1) quantify the observed uncertainty in 5 sets of published station velocities, 2) quantify differences between observed and published uncertainties, 3) assess the extent velocity differences are consistent with different velocity estimations versus consistent with different underlying GPS positions, and 4) assess whether the variability in published velocity solutions is random or correlated with the degree of active surface deformation.

2 Published GPS products

We analyze three-component North/East/Up (NEU) daily GPS positions and the associated secular velocity estimates from 4 analysis centers: the Geodesy Advancing Geosciences and EarthScope (GAGE) at Massachusetts Institute of Technology, Scripps Orbit and Permanent Array (SOPAC) at Scripps Institution of Oceanography, NASA Jet Propulsion Laboratory (JPL) in Pasadena, CA, and Nevada Geodetic Laboratory at the University of Nevada Reno (UNR). These 4 centers produce 5 independent position/velocity datasets (or “solutions”), which are the basis of the analysis. We occasionally refer to the north and east together as the “horizontal” directions and the up as the “vertical” direction.

The “GAGE” solutions in our analysis (Herring et al., 2016) were produced using GLOBK software to combine independent daily position solutions generated by the GAMIT (Herring et al., 2015) and GIPSY OASIS II (Zumberge et al., 1997) packages. SOPAC and JPL provide independent position solutions to the NASA MEaSUREs Solid Earth Science Data Records project. The “MEASURES-JPL” solution is processed using GIPSY and the “MEASURES-SOPAC” solution is processed using GAMIT, and a combination of both solutions (Bock et al., 1997) is available from NASA as the “JPL” solution. The “UNR” solution is produced by the Nevada Geodetic Laboratory, which uses GIPSY to process daily positions for >17,000 GPS stations around the globe (Blewitt et al., 2018). While only 2 software packages are used, each analysis center parameterizes its processing in a unique way and applies different auxiliary models and assumptions (e.g. to characterize atmospheric delay along the signal path from GPS satellite to GPS station). Furthermore, each analysis center applies a different algorithm to estimate published station velocities.

Our study considers 580 GPS stations located in a tectonically active region of the western U.S.A. (30.25˚ to 41.25˚N, 118.25˚ to 121.0˚E). We use published position time series and velocities in the IGS08 reference frame for these stations for all 5 solutions (GAGE, MEASURES-SOPAC, MEASURES-JPL, JPL, and UNR; see Supporting Information). The start time, and therefor the timespan, of the position data is variable for each solution, with many PBO sites coming online in 2006, and the end time is early 2019 when the records were accessed. Additionally, we produce two standardized velocity datasets by uniformly applying two of the velocity estimation techniques (described below) to daily positions from each of the analysis centers using the entire record of published solutions. This allows us to separately attribute the variability in published velocities to differences between 1) position estimates and 2) velocity algorithms.

3 GPS preprocessing and time series analysis

3.1 Removal of offsets and outliers in GPS position time series

Decadal-length continuous GPS time series such as those we analyze in this study typically include one or more step-like offsets caused by equipment changes or earthquakes, position outliers from system or environmental noise, and/or temporal gaps from equipment malfunction or scheduled maintenance. We use metadata provided by the Nevada Geodetic Laboratory (Blewitt et al., 2018) to provide the time of potential offsets for each GPS station, assuming that any remaining offsets are insignificant. We model potential offsets as a Heavyside step function in all three coordinate directions, which we scale by the difference between the median positions of the 14 days before and after the offset time. We subtract all estimated offsets for each GPS station to generate offset-corrected time series for further analysis.

To identify outliers in each station time series, we calculate and remove a 6-month moving average from offset-corrected NEU positions, then calculate the median-average-deviation of the residuals in each coordinate direction. Outliers are defined as epochs whose residual value in any coordinate direction exceeds 5 times the associated deviation. The 6-month window length is selected to capture expected seasonal and longer-period signals, while identifying shorter-period variability (e.g. periodic snow cover on GPS antennas) in the outlier estimation. Outliers, which typically occur at a few isolated days, are replaced by their corresponding values from the 6-month moving average. Since our analysis of velocities does not require complete time series, we do not estimate or otherwise provide position values for time series gaps.

3.2 Time-series velocity estimates

We use two methods to generate NEU velocity estimates for the 5 published position solutions. The first method ("MIDAS") applies the non-parametric MIDAS algorithm, which utilizes median statistics to estimate robust velocities from the offset/outlier-corrected time series (Blewitt et al., 2016). The second method ("parametric") obtains velocities from Equation 1.

$$x(t) = c_1 + c_2 t + \sum_{n=1}^{2} (a_n \sin 2\pi t n + b_n \cos 2\pi t n) \quad (1)$$

The observed time series $x(t)$ is modeled as a mean value c_1, a linear velocity $c_2\, t$, and annual and semiannual sinusoids with coefficients (a_1,b_1) and (a_2,b_2), respectively. While we do not use the sinusoid terms in our analysis, including them in the model ensures that our velocity estimates are not biased for time series that span a non-integer number of sinusoidal cycles. We solve Equation 1 using robust linear least squares to derive model coefficients that minimize the misfit between the observed and modeled time series.

3.3 Ensemble GPS vertical velocity field

We use the GPS imaging method (Hammond et al., 2016) to estimate the vertical velocity field associated with station velocities from each analysis center, interpolating the results onto a uniform 0.1˚ grid (Figure S1a-e). Working with velocity fields rather than individual stations mitigates the impact of station-specific noise, which can obscure the underlying spatial structure of deformation (Hammond et al., 2016; Kreemer et al., 2018). We create an ensemble velocity field for California (Figure S1f) whose individual realizations are estimated by randomly selecting a velocity value for each GPS station from one of the 5 analysis centers. The process is repeated 1000 times and the mean of all iterations for each grid cell is the ensemble velocity field and the standard deviation estimates the uncertainty. The results do not considerably change when using more iterations.

4 Results

4.1 Solutions for each processing center

4.1.1 Published velocities

To assess aggregate differences between analysis centers, we compare the published GPS station velocities for each station relative to the mean of the station velocities from all five centers (henceforth "mean velocity"). Our analysis uses the robust sample statistics of the station-by-station residuals calculated by subtracting the mean velocity from published velocities in the NEU directions. We use the median of the residuals to evaluate their central tendency and assign the robust standard deviation (SD) of the residuals to 0.74 of the interquartile range, to quantify the dispersion (Table 1). Residual velocities relative to their mean range from -0.12 to 0.17 mm/yr in the north and -0.10 to 0.06 mm/yr in the east. Similarly, SDs range from 0.19 to 0.26 mm/yr in the north and 0.15 to 0.21 mm/yr in the east. Vertical velocities are more variable than the horizonal, with median values ranging from -0.26 to 0.30 mm/yr and the SD ranging from 0.33 to 0.74 mm/yr.

The distributions of the north and east velocity residuals (Figure S2a/b) show thin tails with 95% of the residuals between ±1 mm/yr, corresponding to the lower SDs reported and indicating good agreement between the analysis centers published horizontal velocities. There is more variability in the up distributions (Figure S2c), with 88% of the residuals ranging between ±1 mm/yr. The GAGE vertical velocities are positively shifted and JPL is negatively shifted relative to the mean, while the others are a factor of 3 smaller. The JPL vertical residuals have the broadest distribution (0.74 mm/yr SD) and no clear central peak.

Table 1. Summary statistics for published, parametric, and MIDAS velocities from 5 analysis centers. The statistics are reported as the median of the velocity residuals (relative to the analysis centers mean) ± the residual robust standard deviation (1σ) in units of mm/yr.

	Published Velocities (mm/yr)			Parametric Velocities (mm/yr)			MIDAS Velocities (mm/yr)		
	North	East	Up	North	East	Up	North	East	Up
GAGE	0.17±0.22	-0.10±0.20	0.30±0.49	0.14±0.10	-0.05±0.09	0.47±0.29	0.11±0.09	-0.01±0.10	0.36±0.22
SOPAC	-0.01±0.26	0.05±0.17	-0.08±0.35	-0.08±0.07	0.01±0.09	-0.07±0.25	-0.12±0.09	0.04±0.09	0.09±0.19
MEAS-JPL	-0.12±0.19	-0.04±0.15	-0.08±0.33	-0.01±0.08	-0.02±0.07	-0.01±0.24	-0.01±0.08	-0.04±0.08	-0.02±0.18
JPL	-0.02±0.24	0.06±0.21	-0.26±0.74	-0.06±0.11	0.06±0.09	-0.34±0.25	0.02±0.08	0.01±0.07	-0.34±0.22
UNR	-0.02±0.20	0.02±0.17	0.08±0.44	-0.00±0.09	-0.01±0.09	-0.05±0.28	-0.00±0.07	-0.01±0.07	-0.07±0.23

The cumulative distribution functions (CDFs) of the published velocities (Figure 1a/c/e) are visually consistent and the distributions are equivalent according to Kolmogorov-Smirnov tests for all pairs of analysis center NEU solutions. Unlike the CDFs of the velocities themselves, the CDFs of reported uncertainties (Figure 1b/d/f) show considerable variability between analysis centers, with much greater differences in the vertical than in the horizontal (by a factor of ~4). In the horizontal, reported uncertainties for the top 30% (east) to 50% (north) of all stations are systematically less than our own empirical uncertainty estimate, defined as the standard deviation (1σ) of the 5 solutions and shown as the black dashed line in the rightmost panels in Figure 1. In the vertical, reported uncertainties are more consistent with empirical uncertainties. The UNR and JPL solutions provide the largest and most realistic uncertainty, with only 25% of the reported uncertainty less than the empirical assessment. We note the UNR reported uncertainty is scaled by a factor of 3 from the calculated value so it is similar to root-mean-square accuracy (Blewitt et al., 2016). The CDFs of velocity uncertainties show that GAGE, MEASURES-SOPAC, and MEASURES-JPL consistently report lower uncertainties than the other analysis centers. Overall, we find that published horizontal uncertainties are underreported relative to our empirical uncertainty estimate, and vertical uncertainties vary by analysis center.

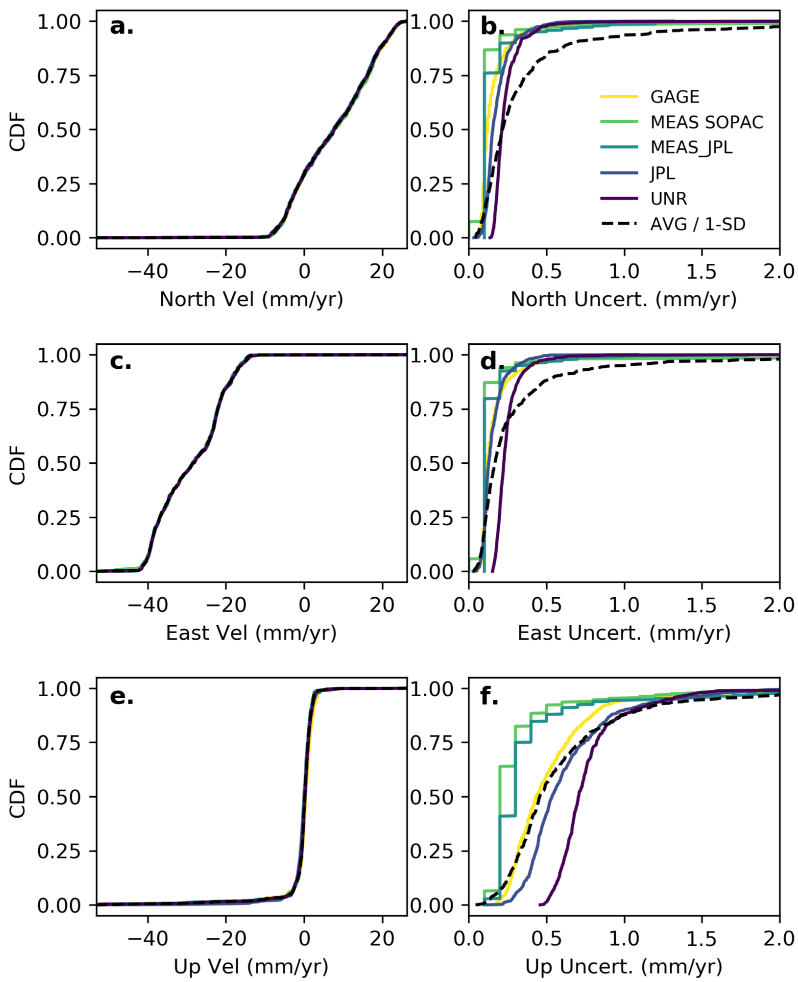

Figure 1. Cumulative distribution functions (CDFs) for the published velocities of the 5 processing centers and reported uncertainties for north (**a** and **b**), east (**c** and **d**), and up (**e** and **f**). The black dashed line indicates the CDF of the mean station velocities (in panels **a**, **c**, and **e**) and the CDF of the 1σ uncertainties of the station velocities (in panels **b**, **d**, and **f**).

4.1.2 Station velocity reanalysis

To understand factors contributing to the velocity differences between analysis centers, we reprocess the GPS station velocities for each center using the two methods described in Section 3.2. Reprocessing velocities using MIDAS reduces the variance (1σ) by ~50% and narrows the range of the residual distributions to about half the values for the published velocities (Figure S3, Table 1). Re-estimating velocities using the time series model in Equation 1 also reduces variance of the residuals relative to the published velocities, but not to the same extent as the MIDAS algorithm (Figure S4, Table 1). The offsets in the means of the up residuals are present in all three velocity estimates (Figures S2c, S3c, S4c) and are a result of the vertical scale estimates applied by each analysis center when obtaining the daily positions (see Herring et al., 2016).

4.2 Vertical velocity assessment

4.2.1 Comparison of station velocities in regions of active deformation

Individual station velocities, averaged across all five analysis centers, reveal clear patterns of deformation across California that serve as context for our analysis below (Figure 2; Dataset S1). The northern Coast Ranges show subsidence of ~1 mm/yr while the central Coast Ranges and Sierra Nevada show uplift of ~2 mm/yr. The Central Valley is subsiding at >50 mm/yr from commercial agriculture groundwater pumping (Faunt et al., 2016) and shows the largest uncertainties in vertical velocity rates. In southern California, south of the Transverse Range, the velocities show a mix of uplift and subsidence that is attributed to tectonic loading and anthropogenic aquifer usage (Argus et al., 2005; Howell et al., 2016). The overall pattern of uplift and subsidence across California is consistent with previous studies of GPS vertical rates (Amos et al., 2014; Hammond et al., 2016), but we identify stations with high velocity uncertainty as reflected in the scatter of published velocity values. Those high-uncertainty GPS stations are primarily located in the high-rate subsidence regions of the Central Valley, Los Angeles basin, and Salton Trough.

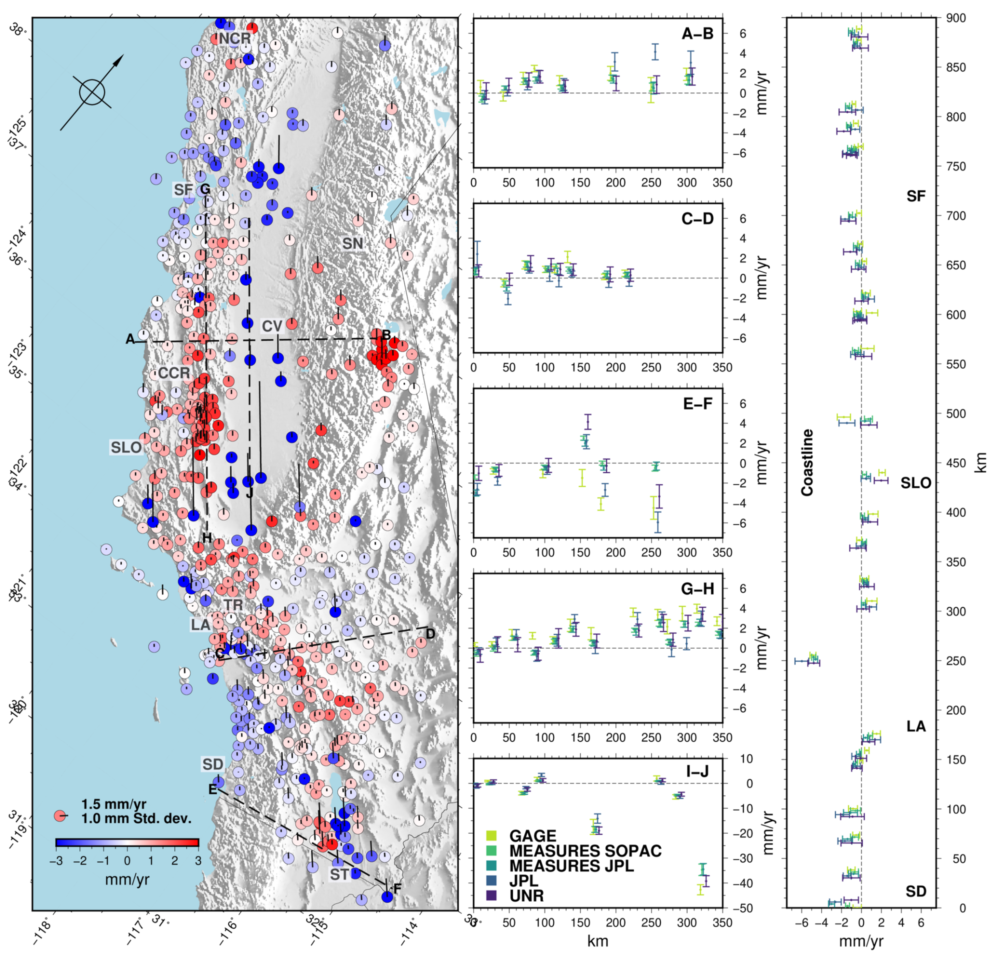

Figure 2. GPS vertical velocities for 5 published processing centers along the coastline and five linear transects in actively deforming regions of California. In the left panel, circle colors indicate published station velocities and the tick mark lengths indicate 1σ uncertainties. In the middle panels, circles and error bars indicate published velocities and 1σ uncertainties. The dashed black lines in the left panel correspond to the ~350 km transects shown in the middle panels. The right panel shows GPS station velocities along the California coast with specific labeled for reference (SF-San Francisco, SLO-San Luis Obispo, LA-Los Angeles, SD-San Diego, CV-Central Valley, TR-Transverse Range, SN-Sierra Nevada, NCR-North Coast Range, CCR-Central Coast Range, ST-Salton Trough).

Vertical velocities along five 350 km transects highlight the differences in the published velocities for areas of known deformation from tectonic, hydrological, and anthropogenic sources (Figure 2). Transect A-B extends from the central Coast Ranges to the Sierra Nevada, excluding measurements in the Central Valley with rapid subsidence. It shows slight subsidence at the coastline, uplift in the Coast Ranges (0.5 to 3.0 mm/yr), and general uplift in the Sierra Nevada (-1.0 to 5.0 mm/yr). Of note, JPL's published velocities for the three stations on the eastern half of the transect are anomalously high by 1~4 mm/yr and uniformly exceed the 1σ uncertainty of the velocity estimates for all other analysis centers.

Transect C-D extends across the Los Angeles basin, crosses the San Andreas fault, and extends into the Mojave Desert. Subsidence in the Los Angeles basin (down to -2.0 mm/yr) is most pronounced near the San Gabriel Mountains, and there is almost no vertical motion in the Mojave Desert. On this transect, JPL published velocities diverge from those of other analysis centers by 1~2 mm/yr, lying outside the 1σ uncertainty of the other velocities for six of eight stations.

Transect E-F extends along the southern U.S. border from San Diego to Yuma, CA, traversing a region of active extensional tectonics. The coastal region shows subsidence (-3.5 to 0.0 mm/yr), the Salton Trough near Brawley, CA shows uplift (1.0 to 5.0 mm/yr), and the eastern Salton Trough shows subsidence (-7.0 to 0.0 mm/yr). This transect is the most problematic from the standpoint of consistency between analysis centers. Four of the 6 GPS station exhibit velocity scatter involving two or more analysis centers and the range of velocities for individual stations (up to 6 mm/yr) is unusually high.

Transect G-H extends north-south along the central Coast Ranges from San Francisco to the southern San Joaquin Valley, following the Hayward-Calaveras-San Andreas Fault system. It shows ~1.0 mm/yr subsidence in the north, with increasing uplift moving south (-1.0 to 4.5 mm/yr). There is some scatter of published velocities, but the uplift trend is similarly represented by all five analysis centers. GAGE velocities are consistently higher than other analysis center velocities along the transect, with the greatest differences (~1 mm/y) toward the south.

Transect I-J extends north-south through the Central Valley with rates to the north near 0.0 mm/yr and strong subsidence (-45.0 to -10.0 mm/yr) at stations in the southern Central Valley caused by agricultural groundwater pumping. While the 2 stations on the transect exhibiting rapid subsidence have the largest scatter in absolute velocity of any station in our analysis, the difference relative to the 1σ velocity uncertainty is better than many other stations.

Motivated by the importance of correctly quantifying vertical land motion near coastal communities in the context of ongoing sea-level rise (National Research Council, 2012), we also examine a transect along the Pacific Coast of California south of Cape Mendocino. The 27 stations in Figure 2 (right panel) show subsidence between San Diego and southern Los Angeles

(-3.0 to 0.0 mm/yr), transitioning to uplift in northern Los Angeles (0.0 to 2.0 mm/yr). Between Los Angeles and San Luis Obispo, subsidence (-6.0 mm/yr) is observed near the agricultural region of Oxnard (250 km), transitioning to a moderate uplift (-1.0 to 3.0 mm/yr). North of San Luis Obispo there is little vertical motion until the San Francisco area, where we observe subsidence (-2.0 to 0.0 mm/yr).

Vertical land motion along California's coast are rarely zero and exhibits areas of local subsidence that can exceed sea level rise by a factor of 2, exacerbating the impact of rising ocean waters. The variability in vertical estimates can be the same order of magnitude as sea level rise, most clearly at stations near San Diego (0~100 km) and San Luis Obispo (450~500 km). This suggests that information about vertical land motion, which is required to inform mitigation efforts to combat rising waters, is dependent on sources whose inconsistencies can result in very different conclusions about what actions may be needed.

4.2.1 Velocity field uncertainty

We use the ensemble velocity field (Figure 3a) and its associated uncertainties (Figure 3b) to highlight regions where differences in analysis center velocities could have the greatest impact on the geophysical interpretation of vertical velocity rates. The dominant features are observed in each analysis center velocity field, but vary spatially with amplitudes differences >3 mm/yr (Figure S1). The highest uncertainties in California are associated with the large-scale subsidence of the southern Central Valley from groundwater pumping for agriculture (Faunt et al., 2016). Subsidence is observed by all analysis centers (Figure S1), however the large variability in reported velocities (Figure 2, transect I-F) and relatively low station density (Figure 3c) both contribute to elevated uncertainties. Another area of high uncertainty is the Salton Trough, which is also subsiding. Median station distance in this area is low (<10 km), indicating that the uncertainty originates entirely from the high variability in station velocity (Figure 2, transect E-F).

The highest uplift rates in California are located in the Sierra Nevada (Figure 3a), a region of somewhat elevated uncertainty (>0.50 mm/yr) that is characterized by low station density and increased uncertainty that results from the anomalously high JPL estimates (Figure 2, transect A-B). However, relatively high uplift rates to the west of the Central Valley are not associated with increased uncertainty. Overall, regions with the highest rates of uplift or subsidence correspond to the largest variance in velocities between analysis centers, but high station density (e.g. to the west of the southern Central Valley) can reduce these uncertainties.

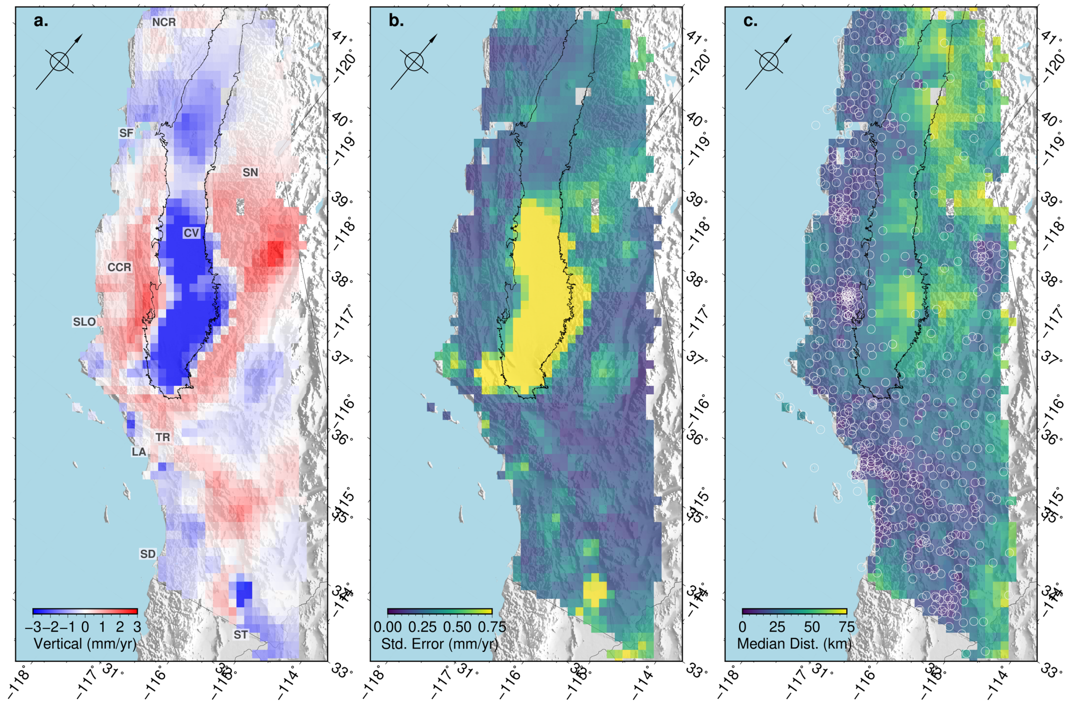

Figure 3. (**a**) The ensemble vertical velocity field and (**b**) standard error computed from all processing center solutions. (**c**) The median distance to GPS stations (white circles) used in imaging each grid; any grid cell with median distance >75 km is removed. The contour outline encompasses the Central Valley where stations are subsiding at rates much greater than -3 mm/yr. Location labels as in Figure 2.

5 Discussion and Conclusions

We analyzed NEU velocities for 580 GPS stations in California, comparing velocity estimates and their corresponding uncertainties from five GPS analysis centers. Taken as a whole, the velocity datasets from different analysis centers are statistically compatible. However, we find differences in vertical rates for individual stations of up to 5 mm/yr between analysis centers, and we document systematic differences in velocities along some transects. Our analysis in Section 4.1.2 shows that these differences arise about equally from different velocity estimation algorithms and different position time series. Velocity differences have implications for the physical interpretation of observed crustal deformation (Figure 2), and care should be taken when using velocities from a single analysis center. One concern is for geophysical models that use uncertainties to weight observations without accounting for the variability introduced by analysis center. An ensemble velocity field such as the one we introduce in Section 3.3 represents one way to reconcile discrepancies in velocity estimates.

The inconsistent reported uncertainties between analysis centers are much larger than the velocities differences themselves. Some are expected based on differences in the methodologies (e.g. Blewitt et al., 2016; Herring et al., 2016) or the applied scale height estimates for the vertical positions (Herring et al., 2016). However, systematic differences are observed in areas of the highest subsidence and uplift (Figure 3), suggesting there are underlying incompatibilities in velocity estimation for these regions. A complication with estimating vertical velocities is the interannual variability in station positions observed as time series increase in length. This non-linear ground motion can result from changes in terrestrial water storage (e.g. Borsa et al., 2014), varying intensity of groundwater usage and recharge (e.g. Neely et al., 2020), and tectonic signals (e.g. Hammond et al., 2018). Both the Central Valley (groundwater) and the Salton Trough (tectonics, groundwater), which we highlight as regions of high variability in vertical velocities, are impacted by strong non-linear surface deformation.

This study provides an independent estimate of NEU velocity uncertainty from the spread between analysis center solutions, both for individual stations and for the ensemble velocity field. We find that published station horizontal velocity uncertainties are systematically smaller than our estimates, while published vertical uncertainties are analysis center dependent. Furthermore, the ensemble uncertainty (Figure 3b) shows that there is a clear spatial pattern in empirical velocity uncertainty. These observations strongly suggest that formal errors from analysis centers do not reflect the true uncertainties of velocity estimates. Ensemble uncertainty estimates, such as the one we introduce here, may provide more realistic values. We conclude that science applications that rely on sub-centimeter GPS accuracy (e.g. assessing sea level rise, InSAR correction and alignment, or hydrogeodetic water storage estimates) should carefully consider and mitigate the inherent uncertainty in published vertical velocity rate estimates.

Acknowledgments and Data

We thank Debi Kilb for insightful comments that improved the manuscript. This material is based upon work supported by the National Science Foundation EAR Postdoctoral Fellowship award 1725344 which supported CWJ. The GPS data products were last accessed 1 April 2019: GAGE from ftp://data-out.unavco.org/pub/products/; MEASURES SOPAC and MASURES JPL from ftp://garner.ucsd.edu/pub/timeseries/measures/ats/; UNR from http://geodesy.unr.edu/index.php; JPL from https://sideshow.jpl.nasa.gov/pub/JPL_GPS_Timeseries/repro2018a/post/point. The composite data sets are available as Supplementary Material Dataset S1.

References

Amos, C. B., Audet, P., Hammond, W. C., Burgmann, R., Johanson, I. A., & Blewitt, G. (2014). Uplift and seismicity driven by groundwater depletion in central California. *Nature, 509*(7501), 483-486. doi:10.1038/nature13275

Argus, D. F., Heflin, M. B., Peltzer, G., Crampé, F., & Webb, F. H. (2005). Interseismic strain accumulation and anthropogenic motion in metropolitan Los Angeles. *Journal of Geophysical Research: Solid Earth, 110*(B4). doi:10.1029/2003jb002934

Argus, D. F., Landerer, F. W., Wiese, D. N., Martens, H. R., Fu, Y., Famiglietti, J. S., et al. (2017). Sustained Water Loss in California's Mountain Ranges During Severe Drought From 2012 to 2015 Inferred From GPS. *Journal of Geophysical Research: Solid Earth, 122*(12), 10,559-510,585. doi:10.1002/2017jb014424

Blewitt, G., Hammond, W. C., & Kreemer, C. (2018). Harnessing the GPS data explosion for interdisciplinary science. *Eos Trans. AGU, 99*. doi:10.1029/2018EO104623

Blewitt, G., Kreemer, C., Hammond, W. C., & Gazeaux, J. (2016). MIDAS robust trend estimator for accurate GPS station velocities without step detection. *Journal of Geophysical Research: Solid Earth, 121*(3), 2054-2068. doi:10.1002/2015jb012552

Bock, Y., Wdowinski, S., Fang, P., Zhang, J., Williams, S., Johnson, H., et al. (1997). Southern California Permanent GPS Geodetic Array: Continuous measurements of regional crustal deformation between the 1992 Landers and 1994 Northridge earthquakes. *Journal of Geophysical Research: Solid Earth, 102*(B8), 18013-18033. doi:10.1029/97jb01379

Borsa, A. A., Agnew, D. C., & Cayan, D. R. (2014). Ongoing drought-induced uplift in the western United States. *Science, 345*(6204), 1587-1590. doi:10.1002/wrcr.20173

Dixon, T. H. (1991). An introduction to the Global Positioning System and some geological applications. *Reviews of Geophysics, 29*(2), 249-276.

EarthScope O&M Proposal. Retrieved from www.earthscope.org/about/printed_documents.html:

Faunt, C. C., Sneed, M., Traum, J., & Brandt, J. T. (2016). Water availability and land subsidence in the Central Valley, California, USA. *Hydrogeology Journal, 24*(3), 675-684. doi:10.1007/s10040-015-1339-x

Fu, Y., Argus, D. F., & Landerer, F. W. (2015). GPS as an independent measurement to estimate terrestrial water storage variations in Washington and Oregon. *Journal of Geophysical Research: Solid Earth, 120*(1), 552-566. doi:10.1002/2014JB011415

GAGE Facility Proposal. Retrieved from www.unavco.org/highlights/2018/award.html:

Hammond, W. C., Blewitt, G., & Kreemer, C. (2016). GPS Imaging of vertical land motion in California and Nevada: Implications for Sierra Nevada uplift. *Journal of Geophysical Research: Solid Earth, 121*(10), 7681-7703. doi:10.1002/2016jb013458

Hammond, W. C., Burgette, R. J., Johnson, K. M., & Blewitt, G. (2018). Uplift of the Western Transverse Ranges and Ventura Area of Southern California: A Four-Technique Geodetic Study Combining GPS, InSAR, Leveling, and Tide Gauges. *Journal of Geophysical Research: Solid Earth, 123*(1), 836-858. doi:10.1002/2017jb014499

Herring, T., King, R., & Mcclusky, S. (2015). Introduction to GAMIT/GLOBK, Release 10.6. Massachusetts Institute of Technology.

Herring, T. A., Melbourne, T. I., Murray, M. H., Floyd, M. A., Szeliga, W. M., King, R. W., et al. (2016). Plate Boundary Observatory and related networks: GPS data analysis methods and geodetic products. *Reviews of Geophysics, 54*(4), 759-808. doi:10.1002/2016rg000529

Howell, S., Smith-Konter, B., Frazer, N., Tong, X., & Sandwell, D. (2016). The vertical fingerprint of earthquake cycle loading in southern California. *Nature Geoscience, 9*, 611. doi:10.1038/ngeo2741

Johnson, C. W., Fu, Y., & Bürgmann, R. (2017). Seasonal water storage, stress modulation, and California seismicity. *Science, 356*(6343), 1161-1164. doi:10.1126/science.aak9547

Kreemer, C., Hammond, W. C., & Blewitt, G. (2018). A Robust Estimation of the 3-D Intraplate Deformation of the North American Plate From GPS. *Journal of Geophysical Research: Solid Earth, 123*(5), 4388-4412. doi:10.1029/2017jb015257

Leveson, I. (2009). *Socio-Economic Benefits Study: Scoping the Value of CORS and GRAV-D (report for National Geodetic Survey)*. Jackson, NJ: Leveson Consulting.

National Research Council. (2012). *Sea-Level Rise for the Coasts of California, Oregon, and Washington: Past, Present, and Future*. Retrieved from Washington, DC: doi:10.17226/13389

Neely, W. R., Borsa, A. A., & Silverii, F. (2020). GInSAR: A cGPS Correction for Enhanced InSAR Time Series. *IEEE Transactions on Geoscience and Remote Sensing, 58*(1), 136-146. doi:10.1109/TGRS.2019.2934118

Silver, P. G., Bock, Y., Agnew, D. C., Henyey, T., Linde, A. T., McEvilly, T. V., et al. (1998). A plate boundary observatory. *IRIS Newsletter, 16 (2)*, Fall/Winter.

Simpson, R. W., Thatcher, W., & Savage, J. C. (2012). Using cluster analysis to organize and explore regional GPS velocities. *Geophysical Research Letters, 39*(18). doi:10.1029/2012gl052755

Zeng, Y., Petersen, M. D., & Shen, Z.-K. (2018). Earthquake Potential in California-Nevada Implied by Correlation of Strain Rate and Seismicity. *Geophysical Research Letters, 45*(4), 1778-1785. doi:10.1002/2017gl075967

Zumberge, J. F., Heflin, M. B., Jefferson, D. C., Watkins, M. M., & Webb, F. H. (1997). Precise point positioning for the efficient and robust analysis of GPS data from large networks. *Journal of Geophysical Research: Solid Earth, 102*(B3), 5005-5017. doi:10.1029/96JB03860

Earth and Space Science

Supporting Information for

An assessment of GPS velocity uncertainty in California

Christopher W. Johnson[1*], Nicholas Lau[1], and Adrian Borsa[1]

[1]Scripps Institution of Oceanography, University of California San Diego, La Jolla, California, 92093, USA

* Now at Los Alamos National Laboratory

Corresponding author: Christopher W. Johnson (cwj004@ucsd.edu)

Contents of this file

Figures S1 to S4

Additional Supporting Information

Captions for Datasets S1

Introduction

Supplementary figures and data tables used to perform the analysis. The figures provide additional context to the material presented in the main text. The data tables are the published velocities for each processing center compiled for each station that contains a solution at 4 of the 5 processing centers.

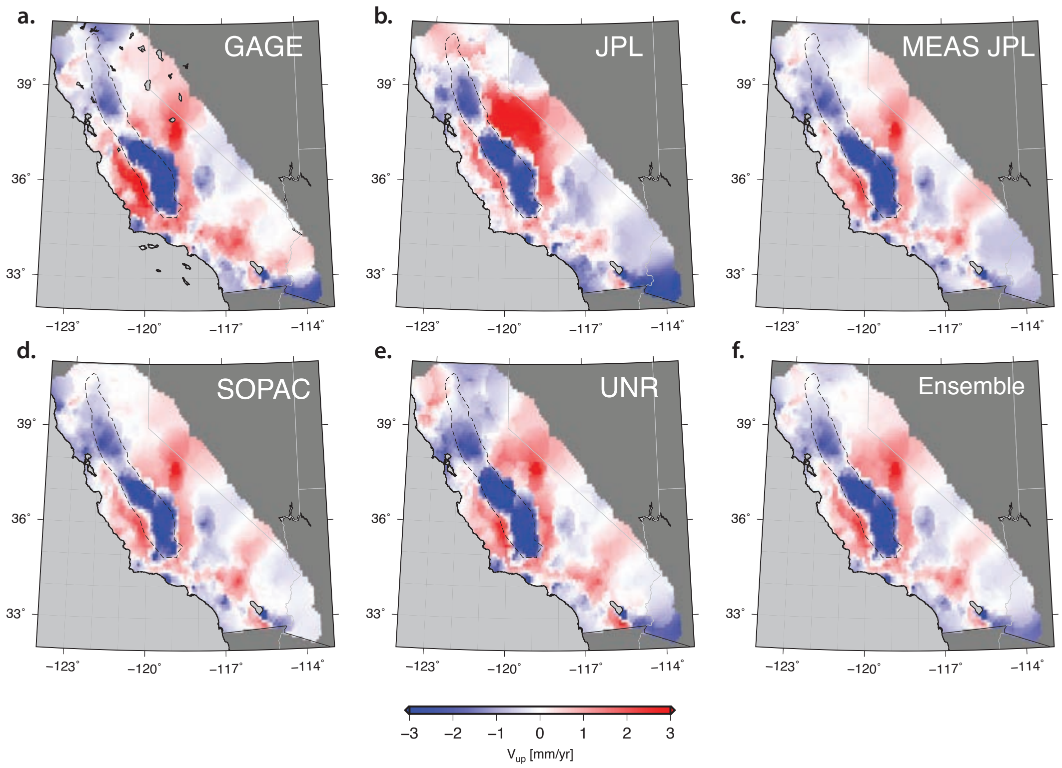

Figure S1. GPS imaging of the vertical velocity field using published values from each processing center. The ensemble velocity field is produced from the mean of 1000 iterations using a vertical velocity randomly selected from a processing center for each station. For reference, the dashed outline encompasses the Central Valley.

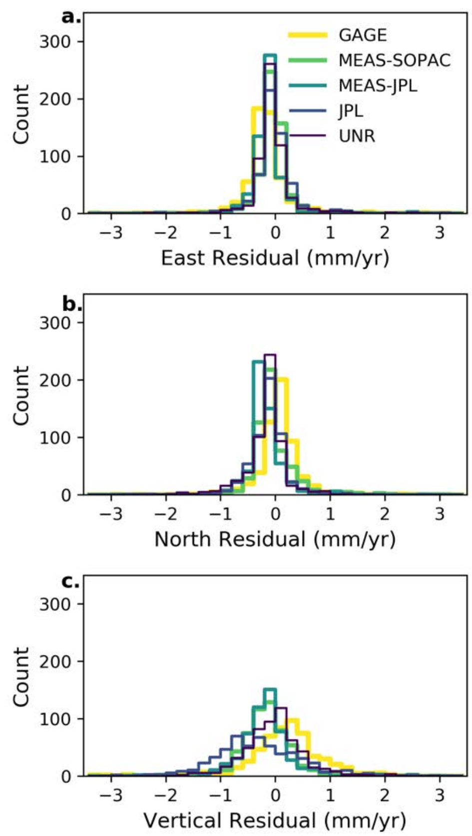

Figure S2. Velocity residual from the average of five processing centers for the (**a**) east, (**b**) north, and (**c**) vertical published values.

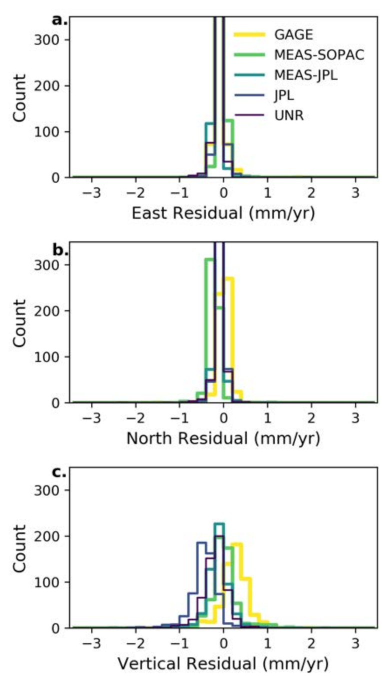

Figure S3. Velocity residual using the MIDAS algorithm for from the average of five processing centers for the (**a**) east, (**b**) north, and (**c**) vertical calculated values.

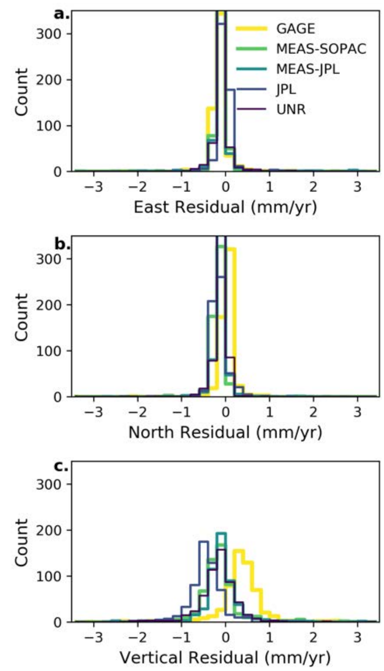

Figure S4. Velocity residual using the time series model in Equation 1 in the main text for the average of five processing centers for the (a) east, (b) north, and (c) vertical calculated values.

Data Set S1. Published velocity values compiled in to a composite velocity data set that contains the station name, longitude, latitude, and north/east/up velocity with empirical uncertainty. The interpolated vertical velocity field with uncertainty includes the longitude, latitude, velocity, and error for the grid.